How Asymmetric Islands Become Symmetric

M. J. Rost, S. B. van Albada, and J. W. M. Frenken
Kamerlingh Onnes Laboratory, Leiden University, P.O. Box 9504, 2300 RA Leiden, The Netherlands
(Received 11 October 2000)

Scanning tunneling microscopy reveals that sputtering of the Au(110) surface results in the formation of vacancy islands with a broken mirror symmetry. These islands exhibit two types of steps on opposite sides: a lower energy (111) step and a higher energy (331) step. We analyze the thermal fluctuations and especially the kink distribution of such vacancy islands. Despite the broken symmetry, which they adopt internally, these islands show a symmetric average outer contour. Their coarsening proceeds via a variety of pathways, often leading to new, symmetric structures, with exclusively (111) steps. The lowest energy vacancy configuration is a bound pair of two vacancy lines or islands.

DOI: 10.1103/PhysRevLett.86.5938 PACS numbers: 68.35.Md, 68.35.Bs, 68.37.Ef, 82.65.+r

Since the invention of the scanning tunneling microscope (STM) it is possible to observe the shapes of atomic-scale objects, such as adatom and vacancy islands, on or in surfaces. The equilibrium shape of such islands is completely determined by the orientation dependence of the step free energy. A graphical form of the relation between the energies and the shape is the well-known Wulff construction [1–4]. The starting point in this construction is a polar plot of the orientation-dependent step free energy. The island shape emerges as the inner contour formed by the full set of lines perpendicular to the vectors from the origin to points on the polar plot. Because the origin of the polar energy plot coincides with the center (of mass) of the island shape, this shape directly reflects the symmetry of the underlying crystal. For example, the "hexagonal" islands with *A*- and *B*-type steps on fcc (111) surfaces exhibit the threefold symmetry of both the fcc crystal and the (111) surface [5]. Sometimes elongated islands are observed [6,7], which do not show the expected equilibrium shape, but this is usually the result of kinetic limitations.

In this Letter we discuss STM observations of islands on the Au(110) surface. In local equilibrium one would expect to find twofold symmetric islands on this surface. Au(110) adopts a missing row reconstruction (MRR), in which every second $[1\bar{1}0]$ atom row is absent (Figs. 1a and 1b), and the crystal and the surface share two mirror planes, namely (001) and $(1\bar{1}0)$. However, in our UHV-STM study on Au(110) we find vacancy islands with only *onefold* mirror symmetry. The symmetry with respect to the (001) mirror plane is broken because each island has two different types of steps on opposite sides: a close-packed step, which we refer to as the (111) step, and a more open step, which we refer to as the (331) step. The Miller indices indicate the orientation of the narrow facet formed by the step atoms. Since the step free energies E_S^{111} and E_S^{331} are significantly different, the origin of the Wulff plot does *not* coincide with the center of mass of the island. Thus we expect asymmetric island shapes. Nevertheless, we find that the islands on Au(110) have a symmetric shape (contour), although their internal structure is clearly asymmetric. We further find that such islands are metastable. Coarsening of regular vacancy or adatom islands, e.g., via Ostwald ripening or coalescence, has been studied intensively, e.g., [8–11], but due to the broken mirror symmetry, the islands on Au(110) reveal a variety of unusual coarsening processes, resulting in more symmetric, lower-energy configurations.

The experiments have been performed with the STM described in [12], at a tunneling voltage of −0.7 V and currents below 0.1 nA. The cleaning procedure of the Au(110) surface can be found in [13]. The removal of 0.2 monolayer (ML) (sputtering with 600 eV Ar^+ ions) from a clean, well-ordered surface at room temperature leads to the formation of vacancy islands that are all 1 ML deep, and have an average length of 100 Å, parallel to the MR direction $[1\bar{1}0]$, and an average width of 40 Å. We find that *all* vacancy islands have a MRR in their interior (Figs. 1a and 1c). This even holds for the narrowest islands with a width of a single MRR period.

As a consequence of the internal MRR, the vacancy islands have a broken mirror symmetry: one of the steps along the MR direction has to be a (111) step (lower step in Figs. 1a and 1c), while the opposite one has to be a (331) step (upper step in Figs. 1a and 1c). This internal asymmetry can clearly be seen in the cross section of Fig. 1b as well as in the line scan of Fig. 1d. The formation

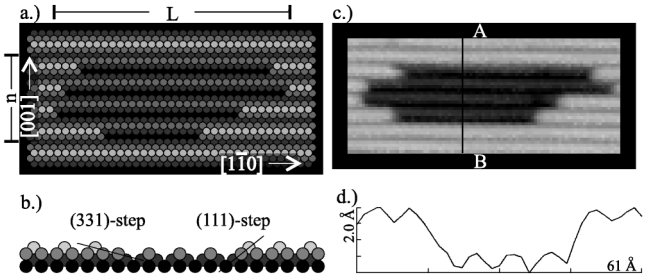

FIG. 1. (a) Schematic top view of a vacancy island with a width of $n = 4$ MRR periods. (b) Schematic cross section. (c) STM image of a vacancy island; the internal MRR is clearly visible. (d) Line scan along *A*-*B* in (c); the (331) and the (111) step can be distinguished easily. Notice the different slopes at the steps. Also notice the asymmetric position of the rows in the island with respect to those on the surrounding terrace.

 0031-9007/01/86(26)/5938(4)$15.00

energies for the (111) and (331) steps have been determined in [13,14]. They amount to $E_S^{111} = 3.7 \pm 0.5$ meV and $E_S^{331} = 15.3 \pm 1.1$ per atomic spacing. We may expect the step *free* energies to exhibit a similarly large difference. This implies that the origin (Wulff point) of the polar plot of the free energy, used in the Wulff construction, does not coincide with the center of missing mass of the vacancy island. The ratio of the step free energies is equal to the ratio of the distances of the steps to the origin of the polar plot. Consequently, it seems natural to expect that the average shape of the perimeter of a vacancy island with its asymmetric internal structure would be strongly asymmetric. However, the average shape that we observe for vacancy islands is completely symmetric. An upper estimate of the asymmetry is presented below. We explain this unexpected result as follows. We describe the formation energy of an island's contour as a simple sum of step and kink energy contributions. We first concentrate on the step energies. The total contour consists of step segments along the $[1\bar{1}0]$ direction, with a length of a single atomic spacing, 2.88 Å, and perpendicular segments along [001], with a length of the MRR period of 8.16 Å. Each $[1\bar{1}0]$ segment has an energy of either E_S^{111} or E_S^{331} (see above). Each [001] segment has an energy of $E_S^{[001]} = 200 \pm 60$ meV [13]. Let L denote the total length of an island along the $[1\bar{1}0]$ direction, measured in atom spacings (see Fig. 1a). We see that the island contains precisely L (331)-step segments as well as L (111)-step segments. Thus it is impossible to reduce the length of the higher-energy (331) step without shortening the (111)-step length by exactly the same amount. As a consequence, the average island contour will not become asymmetric due to a difference between the step free energies E_S^{111} and E_S^{331}.

There are also two different types of kinks. A kink in a (331) step has a formation energy E_k^{331} and a kink in a (111) step has an energy E_k^{111}. If E_k^{331} is lower than E_k^{111} the vacancy islands should contain more (331) kinks than (111) kinks and vice versa. Different amounts of kinks at the two different steps will make one of the sides of the island more rounded and the other more straight, which leads to an asymmetric contour. Following the approach of Ref. [15], we split the energy of each kink E_k^{hkl} into two contributions $E_k^{hkl} = E_S^{[001]} + C_k^{hkl}$, where E_S^{001} again represents the energy of the short [001]-oriented step segment perpendicular to the (111) or (331) step, and C_k^{hkl} is the combined energy of the kink's two corners (convex and concave). If n represents the width of the island in units of the MRR period (see Fig. 1a), the formation energy of the entire island contour can be written as

$$E = L(E_S^{111} + E_S^{331}) + 2nE_S^{[001]} + aC_k^{111} + bC_k^{331}, \tag{1}$$

where a and b denote the numbers of (111) and (331) kinks and $a + b \leq 2n - 2$. We see that it is only via the corner energies of the kinks in the two different steps that the islands can adopt an asymmetric average contour. In 56 STM images each containing nine vacancy islands we have counted in total 722 (331) kinks and 716 (111) kinks. The images were taken at room temperature, at times sufficiently far apart for the islands to rearrange their numbers of kinks. From these numbers we obtain an upper estimate for the difference between the corner energies of $|C_k^{111} - C_k^{331}| < 1.2$ meV. This implies that the energies of the two kink types are equal within 0.6%. It is easy to prove that under more general conditions the Wulff construction produces a twofold symmetric island shape for a onefold symmetric step free energy distribution. Because of the equality of the corner energies, these conditions are indeed fulfilled for (vacancy) islands on Au(110).

It is tempting to apply the inverse Wulff construction to the observed island shape, to derive the full orientation dependence of the step free energy. However, without prior knowledge of E_S^{111} and E_S^{331} the location of the Wulff point is unknown (*not* the island center), and this construction cannot be performed. In addition, the Wulff construction requires the average island shape to reflect thermodynamic equilibrium, which can be verified by observing shape fluctuations of individual islands. Although we have seen rapid fluctuations in the length L of each vacancy island and in the lengths of the individual missing atom rows within each island, none of the islands showed fluctuations in width n, even at 343 K. This probably reflects a high activation barrier for removing an atom from an intact atom row. The lack of width fluctuations does not necessarily imply that the vacancy islands are out of thermal equilibrium, as they can still vary their length, and thereby their aspect ratio, by vacancy or adatom exchange with the terrace. Nevertheless, we will not draw conclusions from the islands' average aspect ratio. Note, however, that the presence of length fluctuations ensures that the analysis presented above of the observed numbers of (111) and (331) kinks remains valid.

We now turn to the coarsening of the asymmetric vacancy islands. Apart from size fluctuations, which led to the occasional disappearance of small islands, we observed three different coalescence pathways and one transformation pathway, dominating the evolution of the surface. (i) Normal coalescence: Two islands reach a more compact shape by fusing together (Fig. 2a). (ii) Slow coalescence: Similar to *i*, but 1 order of magnitude slower (Fig. 2b). (iii) "Bound-pair" formation: Instead of fusing together, two vacancy islands form a bound pair, in which they maintain a small distance along the [001] direction (Fig. 2c). (iv) Transformation of a vacancy island: A single vacancy island spontaneously transforms into two strongly correlated parallel vacancy lines (Fig. 2d). We will refer to this structure as a "bound line pair."

The unusual variety in coalescence pathways (i)–(iii) results from the two basic configurations in which vacancy islands can occur. The interior MRR of a vacancy island

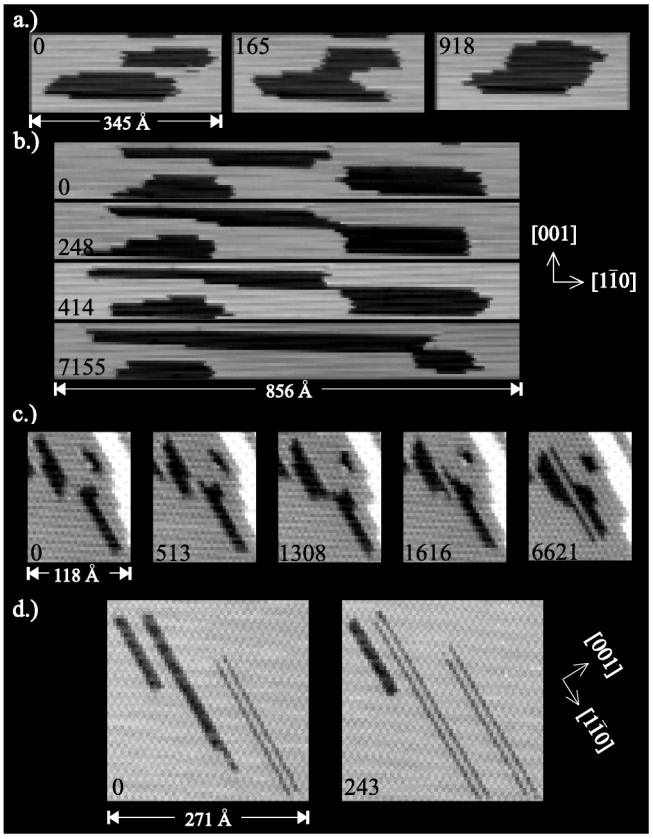

FIG. 2. Annealing sequences of vacancy islands. The time in seconds is indicated in each panel. (a) Normal coalescence $T = 343$ K; (b) slow coalescence $T = 343$ K; (c) "bound-pair" formation; $T = 293$ K. (d) Transformation to a "bound line pair"; $T = 343$ K.

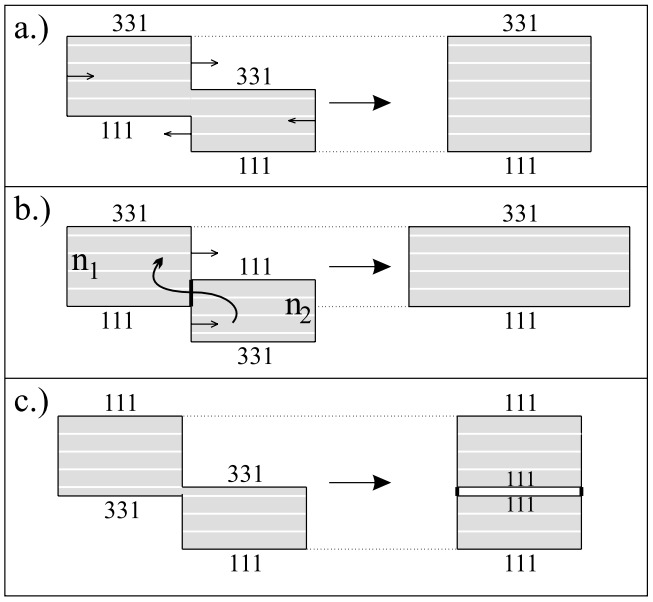

FIG. 3. Three different configurations for the encounter of two vacancy islands. (a) Matching MRR's. (b),(c) MRR's out of phase. In configuration (b) the outer steps are of the high-energy (331) type, while in (c) the outer steps are of the (111) type. The thick lines, connecting the two islands, in the left panel in (b) and in the right panel in (c) indicate domain boundaries in the MRR.

can be adopted by removing either the *odd* atom rows or the *even* rows. This leads to a possible "phase" problem when two vacancy islands meet. If their internal MRR's are in phase, the (111) steps appear on the same side of both vacancy islands. When the islands are out of phase, the (111) step of one island appears on the same side as the (331) step of the other island and vice versa. This leads to three essentially different configurations for two islands meeting each other. In Fig. 3a the internal MRR's of the two vacancy islands are in phase. When this is the case, we observe normal (i.e., rapid) coalescence (Fig. 2a). Once the islands are connected, the connection rapidly widens, which lowers the energy by up to $E_S^{111} + E_S^{331} = 19$ meV per atomic spacing. This involves mainly diffusion of Au atoms along the fast $[1\bar{1}0]$ diffusion direction. When the MRR's of the two vacancy islands are out of phase (Figs. 3b and 3c), we observe either slow coalescence (Figs. 2b and 3b) or bound-pair formation (Figs. 2c and 3c). We have never observed that one of the two vacancy islands switched the phase of its interior MRR in order to come into registry with the other island, even at temperatures up to 400 K. Figure 3b shows the starting configuration for the slow coalescence. Because the two islands are out of phase, a domain boundary is formed between them (see thick line in left panel of Fig. 3b). We observe that the domain boundary remains located at the narrow neck connecting the two islands, where it is shortest and costs the least amount of energy. The clear preference for islands to stay in touch in this configuration (Fig. 2b) demonstrates that $E_{DB}^{[001]} < 2E_S^{[001]} = 400 \pm 120$ meV per MRR period. There are several potential reasons for the dramatic difference between the coalescence time scales in Figs. 2a and 2b. From the position of the narrow neck in Fig. 2b one sees that the slow coalescence takes place by motion of the domain boundary (in this case from left to right), which moves hand in hand with the transport of Au atoms between the islands (indicated by the curly arrow in Fig. 3b). This increases the length of one of the two islands at the expense of the other. How much the total energy changes on average when a single Au atom is moved over the boundary; in other words, the driving force for the motion of the boundary depends on the widths n_1 and n_2 of the two islands. When $n_1 = n_2$, there is no change in energy, and the boundary performs an unbiased random walk. When the widths are not equal, the energy change equals $\frac{|n_1 - n_2|}{n_1 n_2}(E_S^{111} + E_S^{331})$; for differences $|n_1 - n_2|$ that are not too large, this leads to a much lower driving force than that of the matching vacancy islands in Fig. 2a. Kinetic limitations also contribute to the difference in coalescence times. The coalescence of nonmatching islands involves substantial diffusion along the [001] (cross-channel) direction, which is known to be slow [16]. Matching islands merge mainly via diffusion along the fast

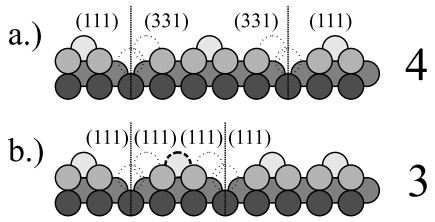

FIG. 4. Schematic cross sections: (a) Two vacancy islands before transforming into a bound pair. (b) Bound pair. For both structures, the number of atom rows missing with respect to the perfect MRR is indicated on the right.

$[1\bar{1}0]$ (in-channel) direction. In addition, all transport between the nonmatching islands proceeds only via the narrow neck. Finally, the domain boundary might act as an extra diffusion barrier for Au atoms between the connected vacancy islands, thereby slowing down the coalescence for out of phase vacancy islands even further.

It is easy to see why the geometry of Fig. 3c leads to the bound-pair formation. Again, the MRR's are out of phase. But now the two islands can replace their two (331) steps by two (111) steps. The rearrangement of the two (331) steps is illustrated in the cross sections of Fig. 4. Initially, the two vacancy islands face each other with (331) steps (Fig. 4a). At the vertical lines additional MRR unit cells can be inserted to obtain vacancy islands with larger widths. Figure 4b shows the alternative configuration with the two (331) steps transformed into two (111) steps. Notice that the MRR's on both sides of the vacancy island pair in Fig. 4b remain in phase with each other, whereas the atom row (dashed) between the two islands is out of phase. This causes a short [001] domain boundary at both sides of the island pair (see right panel in Fig. 3c). We estimate that, once initiated, the bound-pair formation process lowers the energy of the configuration by $2(E_S^{331} - E_S^{111}) - 4E_S^{111}/[2(n_1 + n_2) - 1]$ per transformed atomic spacing. The second term accounts for the difference between the numbers of atoms missing in both configurations, for islands with widths of n_1 and n_2 MR periods. For the depicted case of $n_1 = n_2 = 1$ the estimated energy lowering is 8.3 ± 2.8 meV per transformed atom spacing. The true energy lowering is even higher than this estimate, since lattice relaxations lower the total energy of the configuration in Fig. 4b substantially with respect to $4E_S^{111}$ (see below).

Evidence for this relaxation effect comes from the last restoring pathway: the transformation of individual vacancy islands into bound line pairs. We observe that vacancy islands with a width of 2 MRR periods transform spontaneously into bound line pairs (Fig. 2d). Thus, we conclude that the formation energy of the bound line pair obeys $E_{\mathrm{blp}} < 3/4(E_S^{111} + E_S^{331}) = 14.3 \pm 0.8$ meV. This upper estimate is in the order of 4 times the (111)-step energy $4E_S^{111} = 14.8 \pm 2.0$ meV. The shape fluctuations of bound line pairs have enabled us to obtain a more accurate estimate for this formation energy of $E_{\mathrm{blp}} = 6.0 \pm 3.4$ meV per atomic spacing, which is much lower than $4E_S^{111}$. These observations will be discussed in a future publication. E_{blp} is so low that the peculiar bound line pair structure forms the lowest energy configuration for all vacancy islands with a number of missing Au atoms up to 500. This implies that all vacancy islands of other types, we have observed, have been merely metastable.

We expect analogous shapes and coalescence mechanisms for adatom islands on Au(110). Also other surfaces with (vacancy) islands with a broken symmetry, e.g., due to a MRR, such as Pt(110), Ir(110), and Pd(110), should all exhibit similar behavior. In closing, we note that the situation of equilibrium shapes of which the center does not coincide with the Wulff point cannot occur on the threefold symmetric surfaces, such as fcc (111) surfaces, but is exclusively possible on surfaces with twofold mirror symmetry.

This work is part of the research program of the "Stichting voor Fundamenteel Onderzoek der Materie (FOM)" and is financially supported by the "Nederlandse Organisatie voor Wetenschappelijk Onderzoek (NWO)."

[1] See, e.g., C. Herring, in *Structure and Properties of Solid Surfaces,* edited by R. Gomer and C. S. Smith (University of Chicago Press, Chicago, 1953), p. 5; I. V. Markov, *Crystal Growth for Beginners* (World Scientific, Singapore, 1995), p. 1–41.
[2] D. C. Schlößer *et al.,* Phys. Rev. Lett. **82**, 3843 (1999).
[3] H. P. Bonzel *et al.,* Phys. Rev. Lett. **84**, 5804 (2000).
[4] G. Schulze Icking-Konert *et al.,* Phys. Rev. Lett. **83**, 3880 (1999).
[5] T. Michely and G. Comsa, Surf. Sci. **256**, 217 (1991).
[6] Y. Li *et al.,* Phys. Rev. B **56**, 12 539 (1997).
[7] K. Morgenstern *et al.,* Phys. Rev. Lett. **83**, 1613 (1999).
[8] M. Eßer *et al.,* Surf. Sci. **402–404**, 341 (1998).
[9] W. W. Pai *et al.,* Phys. Rev. Lett. **79**, 3210 (1997).
[10] J.-M. Wen *et al.,* Phys. Rev. Lett. **76**, 652 (1996).
[11] M. S. Hoogeman *et al.,* J. Phys. Condens. Matter **11**, 4349 (1999).
[12] M. S. Hoogeman *et al.,* Rev. Sci. Instrum. **69**, 2072 (1998).
[13] M. J. Rost *et al.,* Phys. Rev. Lett. **84**, 1966 (2000). Note that all step energies in this paper were expressed per lattice constant (4.08 Å). These values were derived on the basis of a theory by E. Carlon *et al.,* Phys. Rev. Lett. **76**, 4191 (1996). More accurate results are obtained using the same theory with more appropriate step entropies. This will be published elsewhere.
[14] M. S. Hoogeman *et al.,* Surf. Sci. **447**, 25 (2000).
[15] B. S. Swartzentruber *et al.,* Phys. Rev. Lett. **65**, 1913 (1990).
[16] F. Montalenti and R. Ferrando, Surf. Sci. **433–435**, 445 (1999).